ENGINEERING TRANSACTIONS • *Engng. Trans.* • **42**, 4, 339–358, 1994
Polish Academy of Sciences • Institute of Fundamental Technological Research

THE FAST CRACK GROWTH ANALYSIS UNDER DYNAMIC LOADING WITH THE HELP OF ADINA

I. V. ROKACH and A. NEIMITZ (KIELCE)

Finite element modelling of dynamic crack growth during impact bend testing is performed using ADINA 6.1. Results are compared with the numerical data reported in literature. The influence of the time step, the Newmark method parameters, types of quadrangular finite elements and form of their mass matrix on the accuracy of dynamic stress intensity factor (DSIF) evaluation is investigated. When numerical damping is not used for some values of the time step, parasitic oscillations of DSIF are registered. Effective methods for elimination of these oscillations are proposed. Conditions for indirect DSIF determination using crack mouth opening displacement are investigated.

1. Introduction

In the last decades, a steady increase of the interest in crack growth modelling is noted. Because of the complexity of the mathematical description of the crack growth phenomenon, almost all of the results for solids of real (that is, finite) geometry were obtained using numerical methods. Among them, the most valuable data were obtained by employing finite element analysis (FEA). The importance of such problems from the practical point of view and the sufficient level of reliability of the corresponding algorithms caused that the crack growth modelling option was included in well-known commercial FEA code ADINA [1]. In the nearest future at least two consequences of this fact may be expected. First, the number of scientists, who can solve the problems connected with crack growth will increase. Second, the existence of a widely accepted software code will partially eliminate the problem of reproducibility of the numerical solutions, and comparison of the results of experimental data processing will be convincing.

The algorithm of crack growth modelling used in ADINA 6.1 has been designed mainly for solving the quasi-static problems. Nevertheless, it may be also used for certain dynamic problems. Unfortunately, direct suggestions how to use ADINA for such problems are not included into the program

manuals [1, 2]. In this paper we have tried to fill this gap partly by estimation of the influence of some computational process parameters on the accuracy of dynamic stress intensity factor (DSIF) $K_I(t)$ evaluation during the fast crack growth modelling in a two-dimensional (2D) solid.

2. Fundamental methods of finite element modelling of crack growth and implementation of this procedure in ADINA

The main difficulty one faces using the FEA in solving crack growth problems is modelling of the continuous changes of boundary conditions on a discrete FE mesh caused by crack tip extension. This problem exists both for dynamic (or unstable), or quasi-static (or stable) crack growth, though in the latter case it is much easier to solve.

There are two different approaches to this problem: using the stationary mesh, or the mesh which is deformed geometrically and periodically remeshed corresponding to the crack extension (see review in [3]). Considering these methods let us assume, for simplicity, that the crack grows along the symmetry axis of the symmetrically loaded 2D solid. This assumption allows us to suppose that the crack is placed along the coordinate axis (Y-axis in Fig. 1), and to consider only a half of the specimen. Boundary conditions in the unbroken portion of the solid on this axis are satisfied by prescribing the displacements to be equal to zero in the corresponding nodes in normal direction (Z-direction in Fig. 1).

According to the first approach, the crack extension is modelled using sequential release of the boundary nodes. Drastic change of solid compliance is preserved by introducing fictitious force in the released node [4, 5]. At the beginning this force is supposed to be equal to the actual reaction in the node. Next, this value is reduced in proportion to the crack tip advance along the FE side. Of course, in such case the boundary conditions on the crack surface are satisfied only approximately.

According to the second approach, any change of the crack tip position is accompanied by a corresponding distortion of the mesh or by the remeshing procedure [3, 6–8]. Here the boundary conditions on the crack surface are satisfied exactly.

In the past, the ADINA users utilized, most often, different versions of the node release method, which may be simply included in any general purpose FE code [9, 10]. Only a few of them used the remeshing procedures for solving more exactly 2D [11, 12] and 3D [13] fracture mechanics problems, after attaching additional subroutines to the program. In the new version of

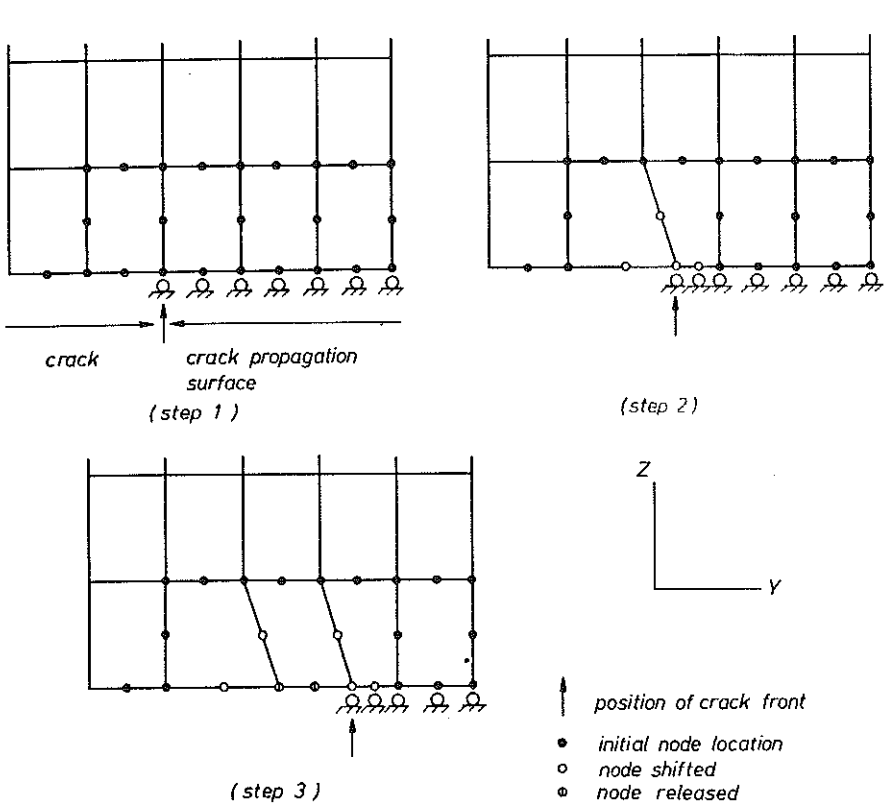

FIG. 1. The node shifting and releasing procedure for crack propagation. (Courtesy ADINA R & D). Nodal conditions along crack propagation surface: Y-direction = free, Z-direction = null prescribed displacement.

ADINA the "node shift/release" technique [12] is applied to 2D modelling of crack propagation. The order of successive changes of a mesh near the tip of a growing crack, according to this technique, is illustrated in Fig. 1. To determine the crack tip position at any load and/or time step, the generalized crack resistance curve is used. This is a user-defined relation between a crack growth control parameter and the crack extension value Δa. As a crack growth control parameter, the node displacement or energy release rate (J-integral) may be used. Other types of this parameter may also be used in the program by the user through Fracture Mechanics Interface.

Depending on the type of crack resistance curve, two different methods of using the FE code may be distinguished. In the first case, the fracture process is modelled by means of the experimentally obtained crack growth history (e.g., in the "grip displacement – crack extension" form). The numerical solution provides values of the parameters, which characterize the stress-strain state near the crack tip (DSIF, J-integral, crack opening dis-

placement or angle, etc.) and which are widely used in different crack initiation and growth criteria. Results of such analysis (so-called "generation phase" [3]) may be used in another phase of calculations, the "application phase". Here the relation between the crack extension and a selected crack growth control parameter (supposed to be a material property) is used for prediction of the crack evolution in the given solid under prescribed mechanical and/or thermal loading.

Standard ADINA capabilities for solving dynamic crack growth problems are limited to the generation phase calculations only. An application phase calculations cannot be performed because, as a rule in dynamic fracture mechanics criteria, the crack growth parameter defines not the crack extension but its velocity.

3. Test problem and the solution method

As a test problem, the crack growth modelling in the 4340 steel beam specimen (length $L = 181\,\text{mm}$, width $W = 38\,\text{mm}$, thickness $15.8\,\text{mm}$) has been used. The specimen was tested on a pendulum testing machine with support span $S = 165\,\text{mm}$ and tup velocity $6.88\,\text{m/s}$ [14]. The crack started from the initial length $a = 9.5\,\text{mm}$, at $t = 95\,\mu\text{s}$ after the first contact between the tup and the specimen, and ran with average velocity of $375\,\text{m/s}$ until $t = 144\,\mu\text{s}$. Then the crack ran with average velocity of $95\,\text{m/s}$ up to the failure of the specimen.

Previously this experiment in a 2D (plane strain) approximation was numerically modelled in [15]. DSIF values were determined directly as internal variables of special motion of the FE [7]. We have considered only one type of boundary conditions for this problem denoted DDT1 in [15]. Here it is assumed that the specimen during a test is in constant contact with both the tup and the supports, and the tup velocity does not change.

For determination of the DSIF two methods were used. In the first one the well-known relation between DSIF and the dynamic analogue of J-integral was used [16]. The latter is determined in ADINA either by contour integration or by the virtual crack extension (VCE) method, used in this work.

As the second approach, the simplified method of Nishioka and Atluri [17] was used. This method is based on the numerically discovered property that the relation between DSIF and the crack mouth opening displacements (CMOD) for impact beam specimens is not essentially sensitive to the crack velocity. For crack growth velocities lower than 15% of the shear wave speed, this relation may be considered to be equal to the static one, with

an error less than 2%. For this case DSIF calculation is reduced to simple multiplication of CMOD values for any time step by the corresponding values of function $A_s(\lambda) = K_I(\lambda)/\mathrm{CMOD}(\lambda)$ determined in statics, where $\lambda = a/W$ is nondimensional crack length.

Two types of FE meshes were used in calculations. The meshes of A-type (see Fig. 2) were used for accurate determination of $A_s(\lambda)$ function values. We had to obtain these values numerically due to nonstandard span-to-width ratio ($S/W = 4.34$) of the specimen. The meshes consisted of Q8 eight-node quadrilateral finite elements. Singularity in the crack vicinity was modelled by shifting the midside nodes of the corresponding elements to the quarter points.

The B-type mesh (see Fig. 3) was used for dynamic crack growth modelling. In this mesh Q8 or Q9 (Lagrangian 9 node) regular FEs were used. Singularity in the crack tip was not modelled (the limitation of implementation of the crack growth modelling technique in ADINA).

There were some differences in the VCE method when it was used for each type of mesh. For A-type meshes, the VCE shift zones consisted of 2 to 5 layers ("semirings") of FEs around a crack tip node. For moving cracks ADINA allows us to use either a moving shift zone or a spatially fixed one. In the first case, the shift zone is linked to the crack tip node and must be defined by the number of "semirings" of FE connected to this node. ADINA selects automatically the elements that belong to the current shift zone. In the second case, numbers of FE in the shift zone are not changed. Hence, this zone must be chosen large enough to include all possible crack tip locations for the problem considered. If the nodal displacement is used as a crack growth control parameter, ADINA permits to use the latter method only. We used three types of VCE shift zones (see Fig. 4) assuming that the nondimensional crack length is within the limits of $\lambda \in [0.25, 0.85]$.

The quality of both meshes and sensitivity of the method of SIF determination to the size of VCE shift zone were tested by solving static problems for three-point bending of the specimen with $\lambda = 0.25\ (0.05)\ 0.85$. Results were compared with the Fett solution [18], obtained by means of the weight functions method for specimens with arbitrary crack length and $S/W > 2$. Error in the SIF determination did not exceed 0.7% for the A-type mesh and 2.5% for B-type mesh, and did not depend on the size of the shift zone.

Simultaneously with SIF, CMOD values were determined and $A_s(\lambda)$ values were obtained. The difference between $A_s(\lambda)$ values obtained on both types of meshes was within 2.5%. For $L/W = 4$, $A_s(\lambda)$ may be derived from the Bakker formulae for $K_I(\lambda)$ and $\mathrm{CMOD}(\lambda)$ [19]. The differences between these data and the results obtained by B-type mesh were less than 2%.

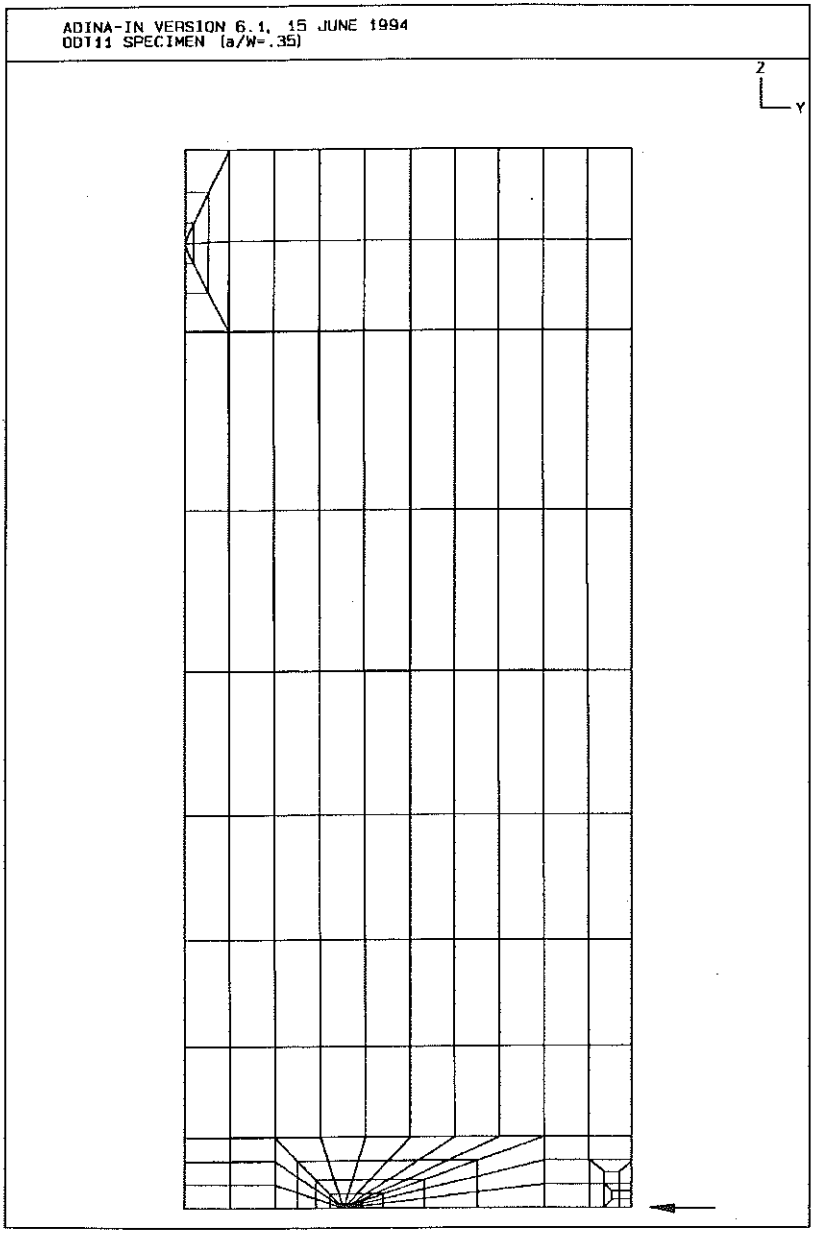

FIG. 2. The A-type mesh (the impact direction is indicated by the arrow).

The dynamic problem for DDT1 boundary conditions was solved using the Newmark time integration method. The specimen deflection Δ in the point of contact with the tup was used as the crack growth parameter.

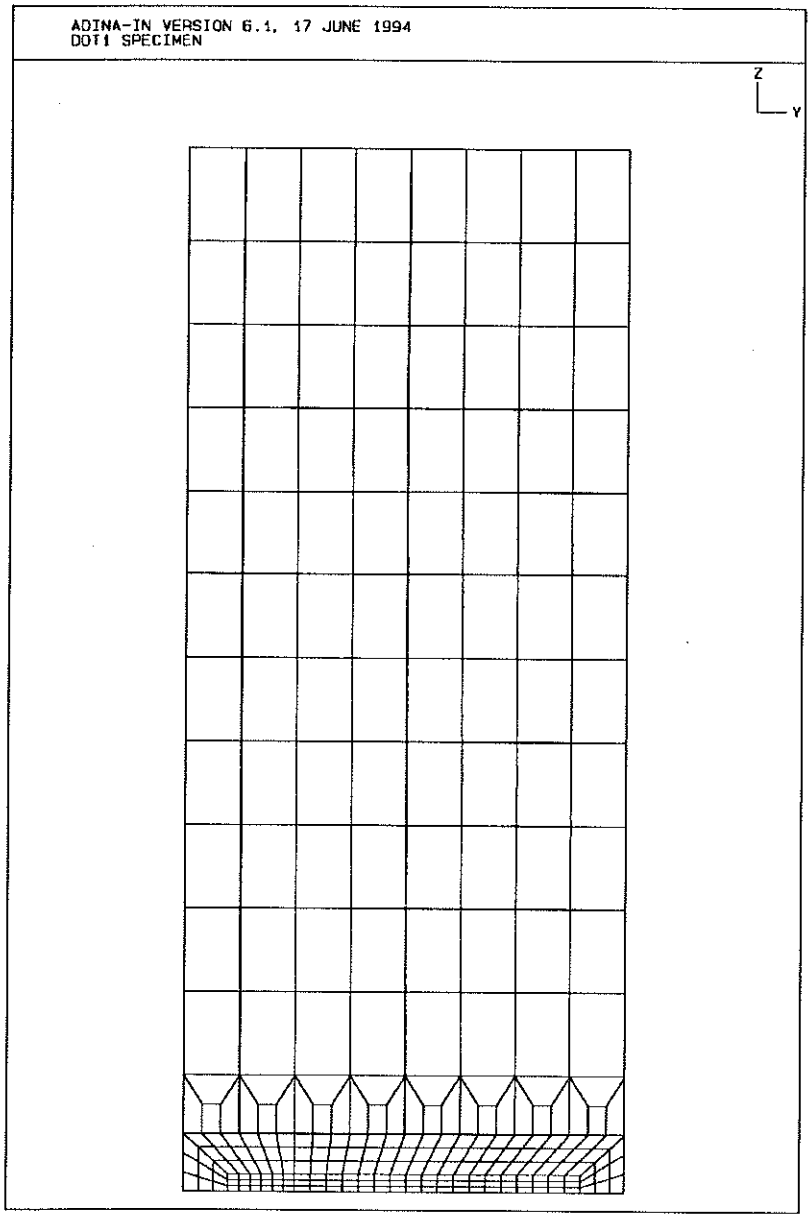

FIG. 3. The B-type mesh.

History of crack growth was described by introducing the piece-wise linear crack resistance curve. According to this curve, the crack was assumed to be stationary ($\Delta a = 0$) for $\Delta < 0.6536\,\text{mm}$ (it corresponds to the moment $t = 95\,\mu\text{s}$ after the beginning of loading). Later the crack length grew linearly.

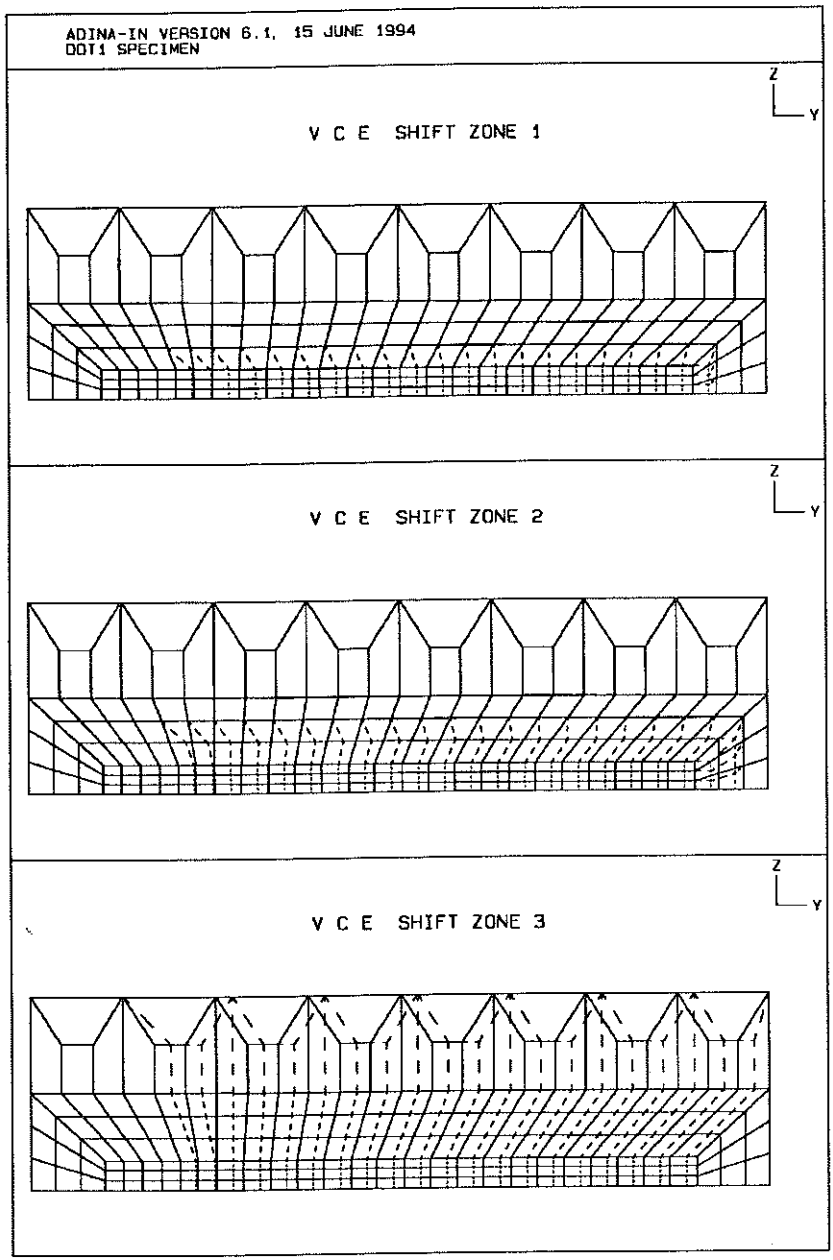

FIG. 4. The VCE method shift zones.

For $\Delta = 0.99137\,\text{mm}$ ($t = 144\,\mu\text{s}$) its extension reached $\Delta = 18.41\,\text{mm}$, which corresponds to the experimentally registered velocity of $375\,\text{m/s}$ and for $\Delta = 1.232\,\text{mm}$ ($t = 179\,\mu\text{s}$) $\Delta a = 21.66\,\text{mm}$ ($95\,\text{m/s}$ for $t > 144\,\mu\text{s}$).

4. Results and discussion

Analysis of the earlier results shows that the parasitic oscillations of DSIF are usually the main source of errors during FEA modelling of crack growth [20]. These oscillations are registered for both the "node release" and "moving mesh" techniques. In the latter case they are caused by interpolation errors corresponding to the remeshing procedure(1). The amplitude of the oscillations may be considerably reduced by utilizing high precision interpolation formulae [21]. It is worth to note that elimination of these oscillations can not be reduced to simple and coarse data filtration or smoothing. These procedures may lead to elimination of important information about physically based drastic changes of DSIF due to the influence of the loading waves on crack propagation.

The influence of the following parameters of numerical solution on the accuracy of DSIF determination and amplitude of its parasitic oscillations has been investigated:

- time step value Δt;
- type of FE mass matrix (MM=L corresponds to the lumped form, MM=C corresponds to the consistent form);
- type of FE (Q8 or Q9);
- VCE shift zone size (notations VCE1, VCE2, VCE3 correspond to zone numbers from 1 to 3 in Fig. 4);
- method of DSIF determination (direct method or using CMOD values).

Time step value

Calculations were performed for $\Delta t = 0.5$, 1, 2, 4 and 6 μs. (For comparison, the dilatation wave travels the distance equal to the smallest FE side in 0.25 μs, crack growth with velocity of 375 m/s requires invoking the remeshing procedure every 3.67 μs).

In Fig. 5 some of $K_I(t)$ curves obtained using ADINA are compared with numerical results of Nishioka *et al.* [15], denoted here and later by $K_{npa}(t)$. For small time step the noticeable $K_I(t)$ oscillations for a running crack have been observed. The character and amplitude of these oscillations are better shown in Fig. 8, where $K_I(t)$ values for $t > 95$ μs are normalized by the corresponding values of $K_{npa}(t)$(2). The mean period of oscillations is about

(1) After each remeshing all data determined in "old" nodes must be recalculated for "new" ones.

(2) Values of $K_{npa}(t)$ used for normalization are not accurate, because they were obtained from piece-wise linear approximation of plots in [15]. Hence, curves in Fig. 8 must be interpreted rather qualitatively than quantitatively.

2 μs, their amplitude reaches maximum for $\Delta t = 1...2\,\mu s$ and practically vanishes after the time step is increased to $\Delta t = 4...6\,\mu s$. However, when time step is increased, the phase error (or period elongation) grows. This phenomenon is commonly observed when the Newmark method is used. It causes the small delays of DSIF responses obtained for larger time steps in comparison to smaller ones (see Fig. 5, 6).

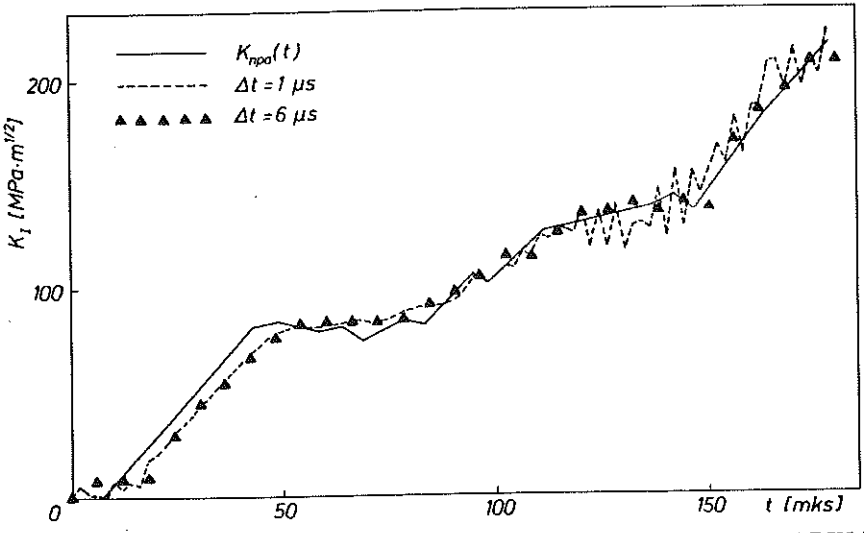

FIG. 5. Comparison of time variation of DSIF obtained in [15] and using ADINA (VCE1, MM = L, $\alpha = 0.25$, $\delta = 0.5$).

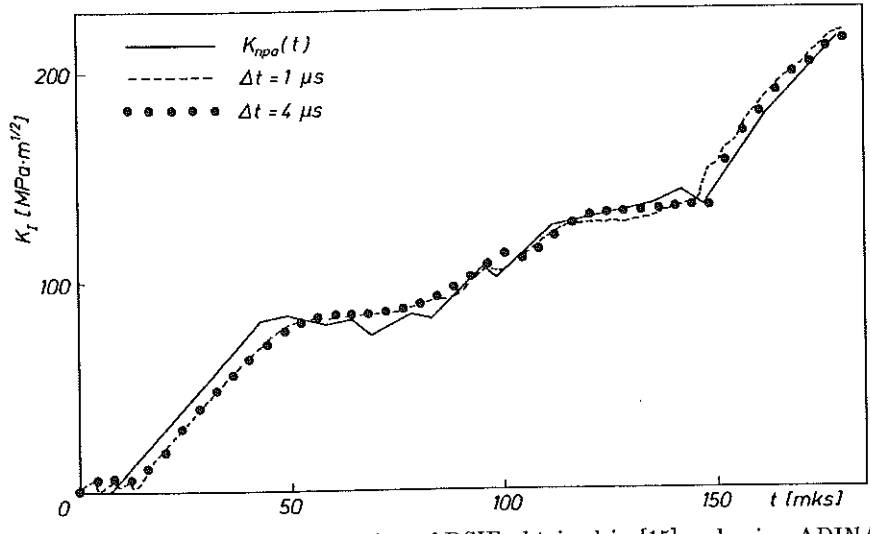

FIG. 6. Comparison of time variation of DSIF obtained in [15] and using ADINA (VCE1, MM = C, $\alpha = 0.5$, $\delta = 0.6$).

Oscillations of DSIF are not the consequence of numerical instability, because the Newmark method is unconditionally stable for $\delta \geq 0.5$. One might assume that the oscillations are connected with high frequency direct and reflected waves of loading. These waves can alter DSIF, and this effect becomes visible only when sufficiently small time steps are used. But even the simplest wave analysis rejects this assumption. These circumstances allow us to suppose that these oscillations are a purely numerical artifact caused by the algorithm of DSIF (more precisely, J-integral) evaluation. There are no oscillations observed for other results of calculations such as CMOD or tup and supports reactions.

Type of FE mass matrix

When the consistent mass matrix is used, the amplitude of DSIF oscillations is reduced in comparison with the lumped MM form (see Fig. 8b). But this replacement did not lead to qualitative changes in numerical results. From the computational point of view, the lumped MM form saves the memory but does not decrease the CPU time.

Type of FE

The most popular serendipity displacement-based FEs are more sensitive to angular distortions than the Lagrangian ones [22]. To obtain maximum accuracy, the serendipity elements should be as nearly rectangular as possible. As shown in Fig. 1, the remeshing procedure utilized by ADINA causes angular distortions of FE near the crack tip. Thus, replacement of conventional Q8 elements by more tolerable to this type of distortion Q9-type elements might lead to noticeable improvement of the results. But real changes in DSIF behaviour were very small if ever (see Fig. 8d).

Numerical damping

Values of the Newmark method parameters used in the calculations discussed above do not provide damping of higher modes of specimen response. Application of a slight damping ($\alpha = 0.5$, $\delta = 0.6$) removes DSIF oscillations for all time steps considered (see Fig. 6, 8b, 8c). At the same time this procedure does not magnify the overall error of DSIF determination and does not change the local variations of $K_I(t)$ connected with the influence of direct or reflected waves of loading.

The VCE shift zone size

We have speculated previously that DSIF oscillations are connected with the procedure of J-integral evaluation only. If this assumption is correct, the numerical damping method may be too rough for removing the DSIF oscillations. In principle, the same result can be achieved by modification of J-integral calculation procedure by the VCE method. There are some indications in the literature as to what kind of modification could be successful here. As it was shown in [20], when the energy release rate was evaluated by the contour integral method, the amplitude of fluctuations of the results decreased with increasing area surrounded by the contour of integration. Similar effect is observed when several elements are moved with a crack tip without distortion during geometrical deformation of a mesh (there is no such option in the procedure implemented in ADINA). If the number of such elements increases, the amplitude of energy release rate oscillations decreases [20]. For the reasons given we may suspect that when dynamic problems are solved (contrary to the static ones), the size of VCE shift zone may affect the accuracy of J-integral determination.

To verify this assumption, DSIF time curves obtained for three different VCE shift zones (see Fig. 4) were compared. It was found that the results for VCE1 and VCE2 zones were almost the same. But when the largest VCE3 zone was used, DSIF fluctuations were practically removed without numerical damping (Fig. 7, 8e). This important result shows that the procedure of increasing the VCE shift zone is the most appropriate method for

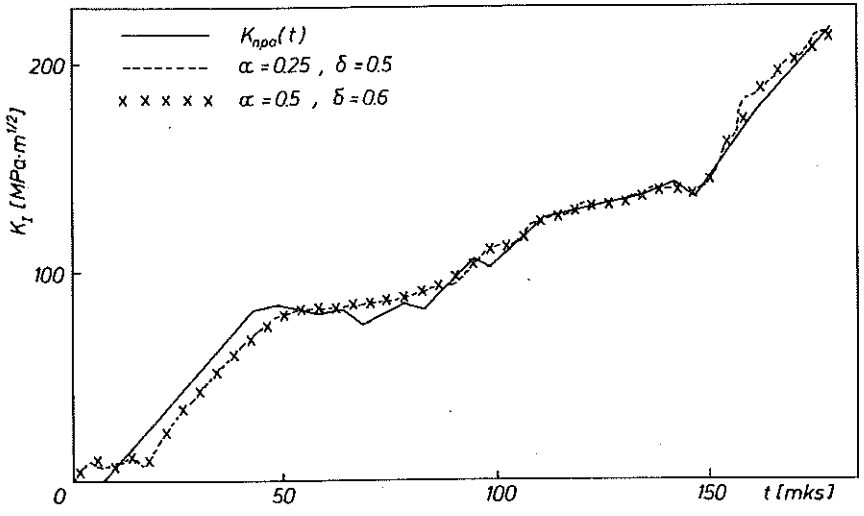

FIG. 7. Comparison of time variation of DSIF obtained in [15] and using ADINA (VCE3, MM = C, $\Delta t = 2\,\mu$s).

elimination of the $K_I(t)$ oscillations. This procedure does not force us to change such global parameters of the computational algorithm as the time step or the Newmark method parameters.

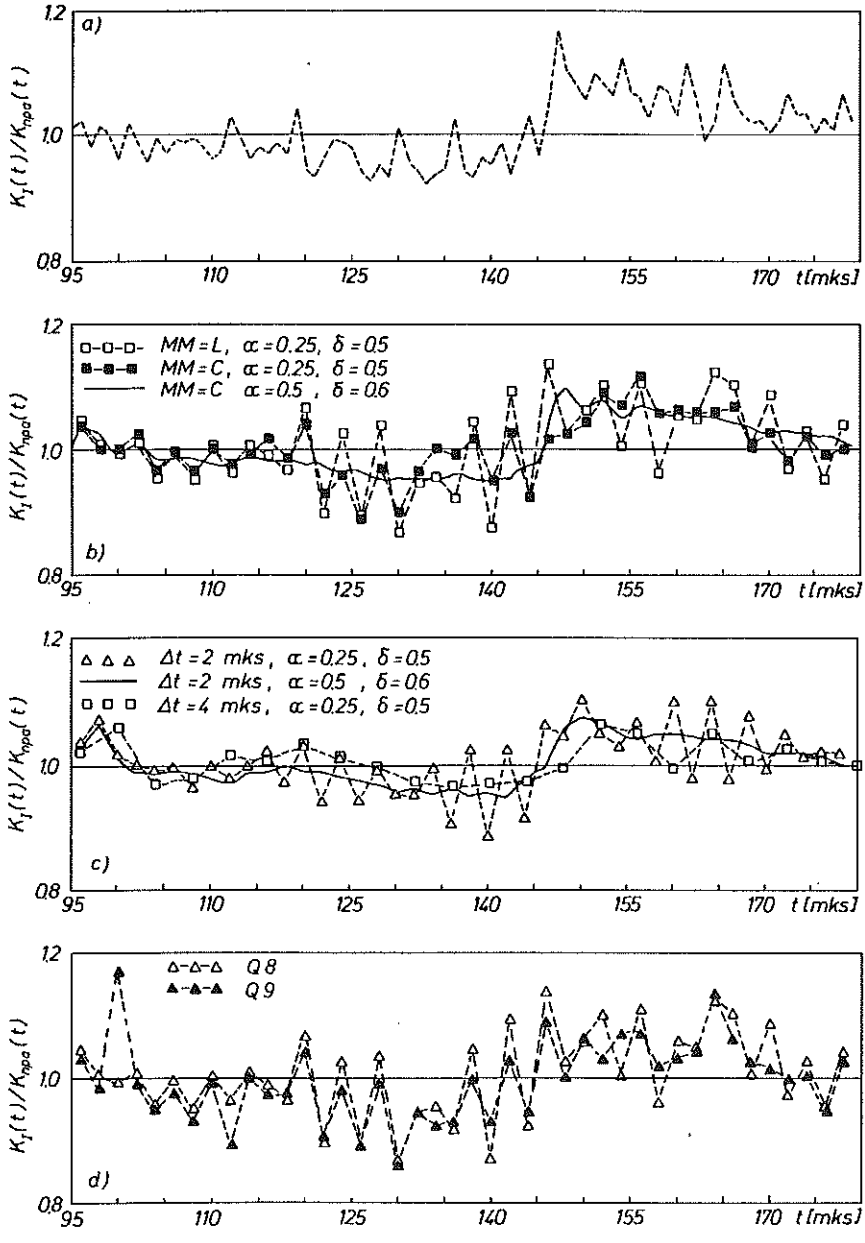

[FIG. 8]

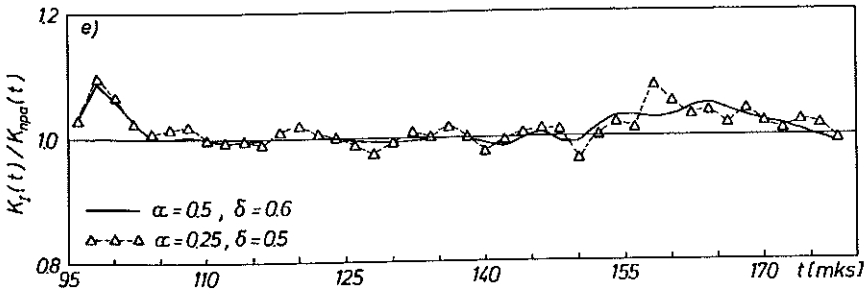

FIG. 8. Normalized time variations of DSIF obtained using ADINA for: a) $\Delta t = 0.5\,\mu s$, MM = L, $\alpha = 0.25$, $\delta = 0.5$, VCE1; b) $\Delta t = 1\,\mu s$, VCE1; c) MM = C, VCE1; d) $\Delta t = 1\,\mu s$, MM = L, $\alpha = 0.25$, $\delta = 0.5$, VCE1; e) $\Delta t = 2\,\mu s$, MM = C, VCE3.

Method of DSIF determination

There are at least two reasons why the determination of DSIF from CMOD values is attractive. First, this method allows us to use more coarse mesh along the crack path. Thus, the time for computations may be considerably reduced. Second, as the authors of this method noticed, it may be useful in experimental practice. Having in mind these circumstances, it is very important to define the limits of applicability of this method.

CMOD for a running crack was determined on B-type mesh. No fluctuations of this value were observed. If the time step is increased, it results in the phase error growth mentioned above (see Fig. 9). But the changes

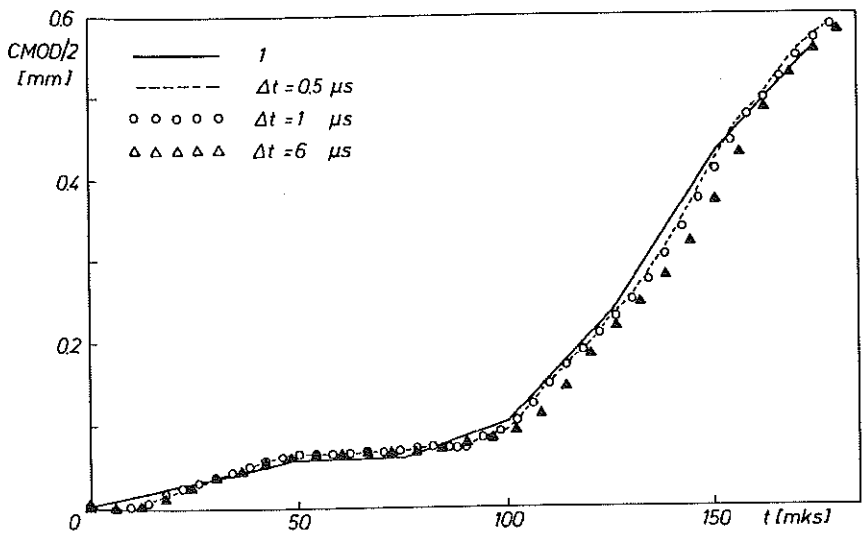

FIG. 9. Comparison of time variation of CMOD obtained in [15] and using ADINA (MM = L, $\alpha = 0.25$, $\delta = 0.5$).

of FE or MM-type and values of the Newmark method parameters have no influence on CMOD.

In Fig. 10 the DSIF values determined directly and indirectly with the time step of 4 μs are compared with $K_{npa}(t)$. All curves were fitted up to the 150 μs ($\lambda \approx 0.75$). Later the indirect results begin to deviate from both the direct ones. Errors in the CMOD(t) and $\Lambda_s(\lambda)$ determination, being very small, can not be the reason for such a considerable divergence. Thus, the indirect approach is of no use here.

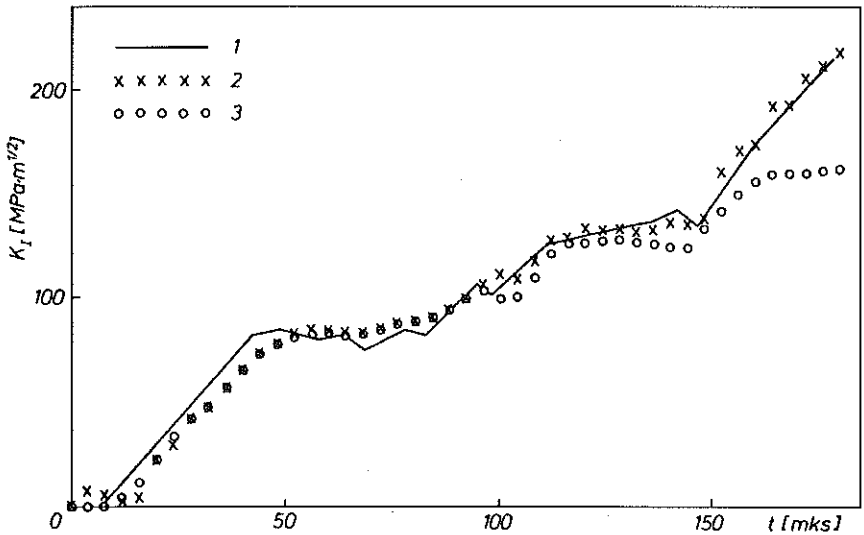

FIG. 10. Comparison of time variation of DSIF obtained in [15] (line *1*) and using ADINA (line *2* – direct calculations, line *3* – indirect method).

The CMOD method is based on an assumption that the $\Lambda_d(\lambda)$ function for a running crack under dynamic loading conditions can be obtained from its static analogue $\Lambda_s(\lambda)$. For the simplest case of the specimen with stationary crack we have

$$\Lambda_d(\lambda) = \Lambda_s(\lambda). \tag{4.1}$$

If the specimen is considered as a linear system, its response to external excitation may be expanded into series with respect to eigenmodes. Hence, both $K_I(t)$ and CMOD(t) may be expanded into such a series too [23]. Let the function $\Lambda_i(\lambda)$ denote SIF to the CMOD ratio for deformation of the specimen according to the i-th eigenmode. The Eq. (4.1) may be satisfied for any dynamic loading and crack length only if

$$\Lambda_s(\lambda) = \Lambda_i(\lambda) \tag{4.2}$$

for $i = 1, 2, \ldots$.

In order to verify the validity of formulae (4.2), the first five symmetrical eigenmodes for the specimen under consideration were determined using ADINA. Two types of boundary conditions (free oscillations and constant contact with the supports) and A-type meshes were used. SIF values for each normalized mode were determined from displacements in the nodes nearest to the crack tip (unfortunately, ADINA does not allow us to use more precise contour integration or VCE method in the modal analysis). According to the results obtained, only $\Lambda_1(\lambda)$ coincides with $\Lambda_s(\lambda)$ (see Fig. 11). For higher

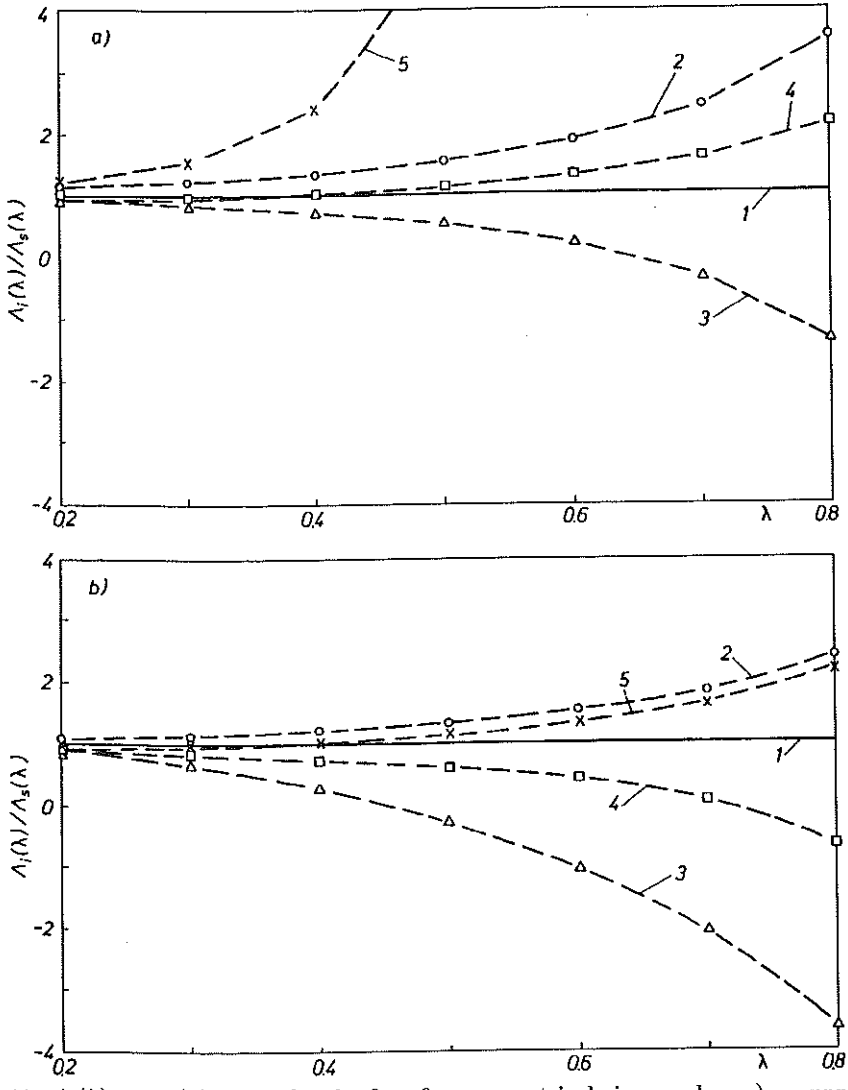

FIG. 11. $\Lambda_i(\lambda)$ to $\Lambda_s(\lambda)$ ratios for the first five symmetrical eigenmodes: a) unsupported specimen; b) simply supported specimen.

modes the divergence between $\Lambda_s(\lambda)$ and $\Lambda_i(\lambda)$ increases with increasing crack length. It means that, even for a stationary crack, employing indirect DSIF calculation method [17] is possible only for such loading, which causes the first mode to be dominant in the specimen response.

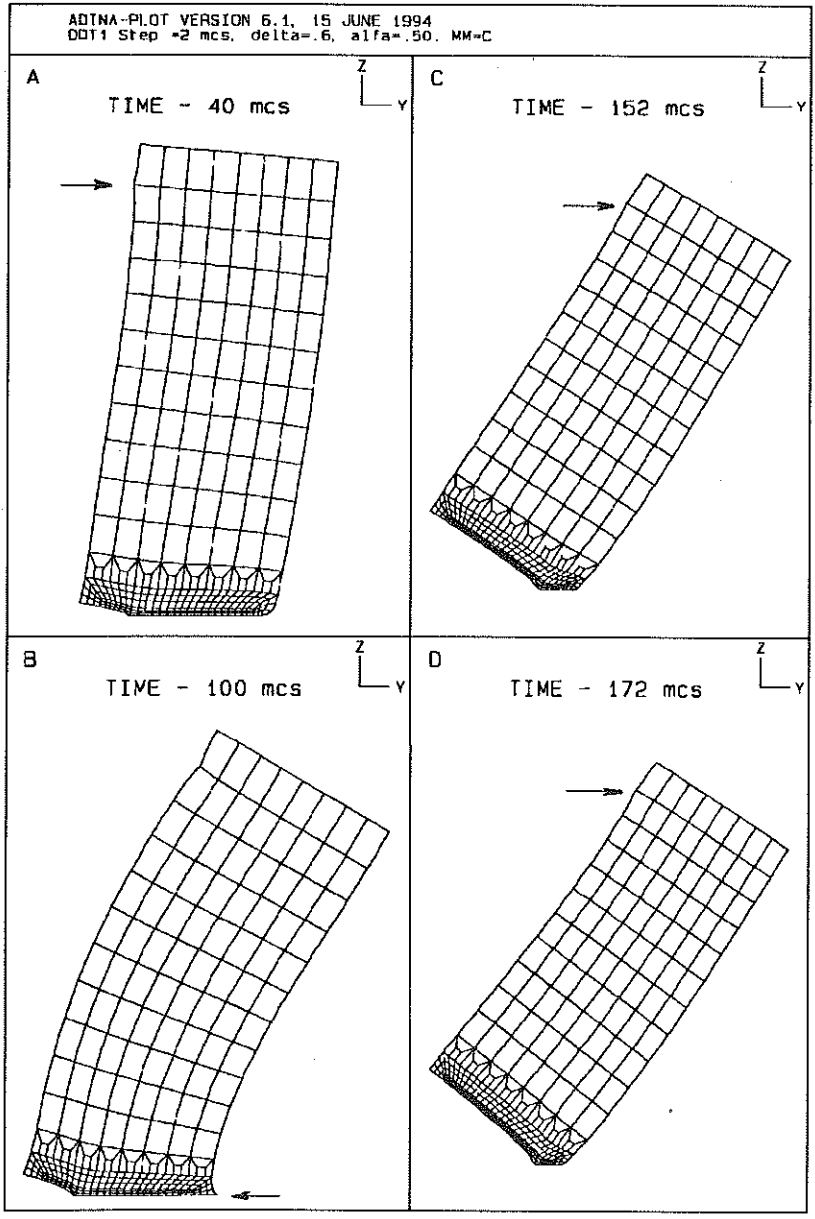

FIG. 12. The deformed specimen shapes at various time moments (magnification factor – 50).

Research programs carried out previously have shown that the first mode of vibration dominates during the one- or three-point bending test [23, 24]. Moreover, this dominance is strengthened when the relative crack length increases. However, these results were obtained for more accurate (one-side contact) boundary conditions (specimen "bouncing" effect was taken into account) than that used in the DDT1 scheme. The assumption concerning the continuous contact of the specimen with the striker and supports causes negative nonphysical reactions to appear. Due to this "sticking" (marked by arrows in Fig. 12), the specimen deformation is altered. The second symmetrical mode oscillations are amplified artificially what results in changes of the specimen concave direction for $t > 150\,\mu s$. This is the reason of divergence between the DSIF values determined by ADINA directly and indirectly.

5. Conclusions

1. Program ADINA 6.1 in the standard configuration allows us to perform dynamic crack growth modelling in generation mode when a displacement in the selected node is used as a crack growth parameter. For the test problem under consideration the accuracy of DSIF determination using the VCE method on coarse regular mesh is comparable with the accuracy that may be obtained using a special moving singular FE.

2. Accuracy of the DSIF determination does not essentially depend on the second order FE type (Q8 or Q9) and their mass matrix type (consistent or lumped).

3. To remove the parasitic oscillations of DSIF, the following methods may be used:

a) the time step increasing;

b) slight numerical damping;

c) increasing of the VCE shift zone size.

The last method seems to be the most efficient.

4. Indirect method of DSIF determination from the CMOD values is valid only for such types of loading which causes the first eigenmode to be dominant in deformation of a specimen.

Acknowledgments

This work was supported by Grant No. 3.0979.91.01 of the Polish State Committee for Scientific Research.

REFERENCES

1. *ADINA theory and modelling guide*, Report ARD 92-8, ADINA R & D. Inc., Watertown 1992.
2. *ADINA verification manual – nonlinear problems*, Report ARD 92-10, ADINA R & D. Inc., Watertown 1992.
3. T. NISHIOKA and S.N. ATLURI, *Computational method in dynamic fracture*, [in:] *Computational Methods in the Mechanics of Fracture*, Ch. 10, Elsevier, Amsterdam 1986.
4. P.N.R. KEEGSTRA, *A transient finite element analysis of unstable crack propagation in some 2-dimensional geometries*, J. Inst. Nucl. Eng., **17**, 4, 89–96, 1976.
5. B. BRICKSTAD and F. NILSSON, *Numerical evaluation by FEM of crack propagation experiments*, Int. J. Fract., **16**, 1, 71–84, 1980.
6. S. AOKI, K. KISHIMOTO, H. KONDO and M. SAKATA, *Elastodynamic analysis of crack by finite element method using singular element*, Int. J. Fract., **14**, 1, 59–68, 1978.
7. T. NISHIOKA and S.N. ATLURI, *Numerical modelling of dynamic crack propagation in finite bodies, by moving singular elements. Part 1: Formulation. Part 2: Results*, Trans. ASME. J. Appl. Mech., **47**, 570–582, 1980.
8. T. NISHIOKA, R.B. STONESIFER and S.N. ATLURI, *An evaluation of several moving singularity finite element models for fast fracture analysis*, Eng. Fract. Mech., **15**, 1–2, 205–218, 1981.
9. B.R. BASS, T.L. KEENEY-WALKER, T.L. DICKSON, C.E. PUGH, C.W. SCHWARTZ and J.C. THESKEN, *Application of ADINA to viscoplastic-dynamic fracture mechanics analysis*, Comp. and Struct., **32**, 3–4, 815–824, 1989.
10. M. IKEDA and T. AIZAWA, *An approach to nonlinear fracture mechanics using ADINA*, Comp. and Struc., **26**, 1–2, 223–231, 1987.
11. H.G. DE LORENZI, *J-integral and crack growth calculations with the finite element program ADINA. Methodology for plastic fracture*, EPRI Contract RP 601-2, 1978.
12. D. SIEGELE and W. SCHMITT, *Determination and simulation of stable crack growth in ADINA*, Comp. and Struc., **17**, 5–6, 697–703, 1983.
13. D. SIEGELE, *3D-crack propagation using ADINA*, Comp. and Struct., **32**, 3–4, 639–645, 1989.
14. M.F. KANNINEN, P.C. GEHTEN, C.R. BARNES, R.G. HOAGLAND, G.T. HAHN and C.H. POPELAR, *Dynamic crack propagation under impact loading*, [in:] *Nonlinear and Dynamic Fracture Mechanics*, ASME Publication AMD, vol. 35, [Eds.] N. PERRONE, S.N. ATLURI, 185–200, 1979.
15. T. NISHIOKA, M. PERL and S.N. ATLURI, *An analysis of dynamic fracture in an impact test specimen*, Trans. ASME. J. Appl. Mech., **105**, 2, 124–131, 1983.
16. S.N. ATLURI, *Path-independent integral in finite elasticity and plasticity, with body forces, inertia and an arbitrary crack face conditions*, Eng. Fract. Mech., **16**, 341–364, 1982.
17. T. NISHIOKA and S.N. ATLURI, *A method for determining dynamic stress intensity factors from measurement at the notch mouth in dynamic tear test*, Eng. Fract. Mech., **16**, 3, 333–339, 1982.

18. T. FETT, *An analysis of the three-point bending bar by use of the weight function method*, Eng. Fract. Mech., **40**, 3, 683–686, 1991.

19. A. BAKKER, *Compatible compliance and stress intensity expressions for the standard three-point bend specimen*, Eng. Fract. Mech., **13**, 2, 145–154, 1990.

20. J.C. THESKEN and P. GUDMUNSON, *Application of a moving variable order singular element to dynamic fracture mechanics*, Int. J. Fract., **52**, 1, 47–65, 1991.

21. T. NISHIOKA and Y. TAKEMOTO, *Moving finite element method aided by computerized symbolic manipulation and its application to dynamic fracture simulation*, JSME Int. J., Ser. 1, **32**, 3, 403–410, 1989.

22. N.S. LEE and K.-J. BATHE, *Effects of element distortion on the performance of isoparametric elements*, Int. J. Num. Meth. Eng., **36**, 20, 3553–3576, 1993.

23. I.V. ROKACH, *A combined numerical/experimental procedure for dynamic stress intensity factor determination in instrumented impact testing*, [in:] *Localized Damage Computer-Aided Assessment and Control*, Southampton, Computer Mechanics Publication, **2**, 179–192, 1990.

24. I.V. ROKACH, *Numerical-analytical analysis of deformation and fracture processes in test specimens under dynamic loading* [in Russian] and [in Polish], PhD thesis, Kielce University of Technology, Kielce 1992.

KIELCE UNIVERSITY OF TECHNOLOGY, KIELCE.

Received July 6, 1994.